Simple Tuning Method of Virtual Synchronous Generators Reactive Control

# Simple Tuning Method of Virtual Synchronous Generators Reactive Control

Fabio Mandrile, Enrico Carpaneto, Eric Armando and Radu Bojoi
*Dipartimento Energia 'Galileo Ferraris'*
*Politecnico di Torino*
Torino, Italy
fabio.mandrile@polito.it

***Abstract*—The integration of renewable energy sources requires new control strategies to make static converters able to provide ancillary grid services, such as virtual inertia and grid support during faults. To address this issue, the idea of making inverters behave as synchronous machines is well known in the literature as the concept of Virtual Synchronous Generator. Thanks to this solution, inverters can provide both inertia and reactive grid support as traditional synchronous machines. However, the tuning of the excitation control of Virtual Synchronous Generator for proper reactive power management has not been properly analyzed in the literature. Therefore, the goal of this paper is to provide a simple tuning criterion for the VSM excitation control with improved dynamic behavior using a feed-forward term. This way, the VSM is able to provide the desired reactive support during faults and quickly track the desired reactive power setpoints. Both a theoretical analysis and experimental tests are provided for a 15 kVA system.**

***Index Terms*—Virtual Synchronous Generator (VSG), Reactive Support, Renewable Integration**

## I. Introduction

The integration of Renewable Energy Sources (RESs) is nowadays one of the goals towards energy sustainability. The challenge consists in guaranteeing the electrical power system stability even in a power electronics-based power system, where most of the power is generated from RESs interfaced to the grid through static converters. To solve this problem, the concept of Virtual Synchronous Machines (VSMs) has been proposed and it is available in the technical literature. The idea is to make a static converter connected to the grid behave as a synchronous generator, in order to provide key ancillary services to the grid, such as virtual inertia and reactive support during grid faults. Even though the literature is rich of insights about VSMs [1]–[6], the analysis of the tuning of the VSM excitation control and its dynamic improvements has not been fully studied. VSM models generally feature one of the following reactive part control:

- Model of the excitation winding of a real Synchronous Generator (SG) and its control [1]. This solution inherits all the disadvantages of real SGs (e.g. transient response of the excitation winding, magnetic couplings, dynamic of the exciter), without leading to better performance;
- A basic reactive droop controller with a simply proportional gain [2];
- A purely integral reactive power controller [5]. In this case a simple tuning formula is given, however neglecting the LC grid interface filter and the effect of the grid itself;
- A Proportional Integral (PI) controller to manage the reactive power flow [7]–[10].

Moreover, no simple formulas are given to tune the parameters of the virtual excitation controllers, starting from the virtual machine and grid connection parameters.

Therefore, this paper deals with a purely integral reactive power controller, with the following goals:

- To provide a simple and straightforward tuning method for the excitation control of VSMs, starting from the virtual machine and grid parameters;
- A feed-forward control to improve the dynamic behavior of the excitation control, decoupling the dynamic behavior of the reactive support against voltage dips in the grid from any reference changes in the reactive power setpoint.

Such feed-forward control is superior compared to using a proportional term in the excitation control both in terms of dynamic response and measurement noise rejection. The applied method is based on a Virtual Synchronous Machine (VSM) implementation available in the literature [11], depicted in Fig. 1, but it can be easily extended to other models.

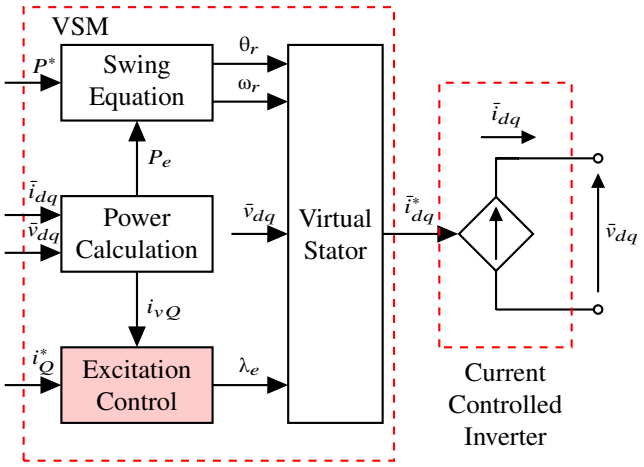


Figure 1. Block diagram of the considered VSM controlling a grid-feeding inverter. This paper analyses the excitation control block, marked in red.

This paper is organized as follows. First, the linearized model used to tune the excitation control gain is described in Section II. Then, in Section III the interaction of the excitation control of the VSM with the reactive current control of the inverter is analyzed. Finally, in Section IV preliminary experimental results are provided.

## II. Linearized Model of the Excitation Control

The VSM here considered generates the current references $\bar{i}^*_{dq}$ for the grid side current-controlled inverter as in Fig. 1. The VSM consists of the following key elements:

1) Swing equation emulation - this block emulates the mechanical behavior of the VSM, regulating the transfer of active power;
2) Virtual stator - this block generates the inverter current references, depending on the measured grid voltage $\bar{v}_{dq}$, the VSM speed $\omega_r$ and the virtual excitation flux linkage $\lambda_e$;
3) Excitation control, marked in red - it is in charge of regulating the exchange of reactive power (or current) and it will be analyzed in this paper.

The considered excitation control is of integral type, as in [5]. In order to simplify the analysis, the following assumptions are made:

1) The connection to the grid is considered mainly inductive, e.g. connection to a medium or high voltage network. Therefore the grid resistance $R_g$ is neglected;
2) Virtual stator resistances are neglected: $R_s \approx 0$;
3) Virtual rotor speed is considered constant $\omega_r \approx \omega_0$ and the linearization is performed around $\omega_0 = 1$ p.u.;
4) Variations of the flux linkages of the virtual machine are negligible $\frac{d\lambda}{dt} \approx 0$;
5) The internal current controller is considered as ideal, since its time constants are much smaller than the ones of the reactive controller;
6) The $d$-axis reactance of the VSM is $X_d$ and the grid reactance is $X_g$, $\lambda_e$ is the virtual excitation flux linkage, $i^*_Q$ and $i_{vQ}$ are the reference reactive current and the actual reactive current of the machine.

Starting from these assumptions, the virtual stator and grid electrical equation can be derived as follows:

$$j\omega_r \bar{\lambda}_{dq} = \bar{e}^{dq}_g + X_g \bar{i}_{dq} \tag{1}$$

where $\bar{\lambda}_{dq}$ is the VSM flux vector, $\bar{e}^{dq}_g$ is the grid voltage vector and $\bar{i}_{dq}$ the current vector injected into the grid by the VSM. All these vectors are defined in the VSM rotor ($d$,$q$) rotating frame.

To analyze the excitation control, only the $d$-axis component of (1) is considered, leading to:

$$\omega_r \lambda_d = e^q_g + X_g i_d \tag{2}$$

The virtual stator can be seen as a Thèvenin equivalent circuit, composed of a voltage source (excitation) and a virtual stator inductance $L_s$ ($X_d = \omega_r L_s$). Therefore, the virtual stator flux $\lambda_d$ can be expressed as:

$$\lambda_d = \lambda_e - L_s i_d \tag{3}$$

By combining (2) and (3), at constant speed $\omega_r = \omega_0$, the equivalent circuit of Fig. 2 is obtained.

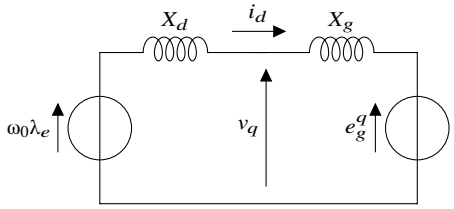


Figure 2. Linearized $d$-axis equivalent circuit of the VSM and the grid.

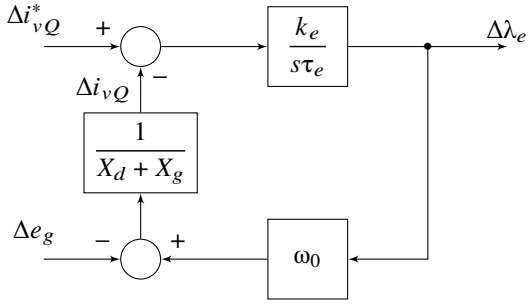


Figure 3. Block diagram of the excitation control of the VSM connected to the grid.

The reactive power exchanged to the grid can be calculated from:

$$Q = v_q i_d - v_d i_q \tag{4}$$

By linearizing (4), assuming the voltage aligned to the $q$-axis and a zero-power operating point ($Q_0 = 0$), the reactive power variation is as follows:

$$\Delta Q = V_{q0} \Delta i_d \tag{5}$$

Therefore, the $d$-axis current $i_d$ is the reactive component of the current, regulating the reactive power exchange. In this paper a reactive current control is considered, therefore $i_d = i_{vQ}$, meaning that the virtual reactive current of the VSG is equal to the $d$-axis current injected into the grid.

From the equivalent circuit of Fig. 2 and the reactive control scheme of the VSG, the block diagram of Fig. 3 is obtained.

The characteristic equation of the equivalent system of Fig. 3 is:

$$s\tau_e(X_d + X_g) + \omega_0 k_e = 0 \tag{6}$$

This system is therefore governed by a single pole with a time constant

$$\tau = \frac{\tau_e (X_d + X_g)}{\omega_0 k_e} \tag{7}$$

This time constant is set by the user to the desired value $\tau = \tau_e$. Therefore, the necessary gain of the excitation control is:

$$k_e = (X_d + X_g)/\omega_0 \tag{8}$$

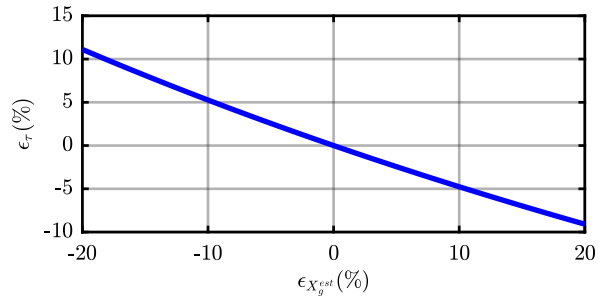


Figure 4. Time constant error $\epsilon_\tau$ due to an estimation error of the grid impedance $\epsilon_{X_g^{est}}$. $X_d = 0.1$ pu, $X_g = 0.1$ pu.

This gain guarantees tunable reactive support with the desired time constant $\tau_e$. The actual time constant depends on the correct estimation of the grid reactance $X_g$. To this purpose, online estimations of the Short Circuit Ratio (SCR) of the grid could be used [12]–[16] to update the excitation control gain dynamically. For most high-power applications, though, the grid impedance is a known value, depending on the point of connection (e.g. Medium voltage connection through known transformer) and can therefore be set as constant.

The error on the actual time constant $\epsilon_\tau$ depends only on the accuracy of the grid impedance estimation $\epsilon_{X_g^{est}}$, since the VSM virtual impedance $X_d$ is set by the user. In fact:

$$\begin{aligned} \epsilon_\tau &= \frac{\tau - \tau_e}{\tau_e} = \frac{\dfrac{\tau_e (X_d + X_g)}{\omega_0 k_e} - \tau_e}{\tau_e} \\ &= \frac{X_d + X_g}{X_d + X_g (1 + \epsilon_{X_g^{est}})} \end{aligned} \tag{9}$$

As it is shown in Fig. 4, this error is almost linear around the ideal estimation point. The influence of the estimation error gets larger as the SCR decreases, therefore proper care must be taken in case of ultra-weak grids.

## III. Interaction with the Inverter Reactive Control

While the reactive support may be desired to act with longer time constants to provide longer current injection, a faster dynamic behavior is expected when the reactive power references are changed by the user. To improve this aspect, a proportional term could be added. However, this term also amplifies any high frequency disturbances that may be present in the feedback system (e.g. measurement noise, harmonics, voltage unbalance). The proposed solution is to add a feed-forward term to predict the necessary excitation flux linkage $\lambda_e$ to guarantee the desired grid reactive current $i_Q^*$ injection. The resulting block diagram is depicted in Fig. 5.

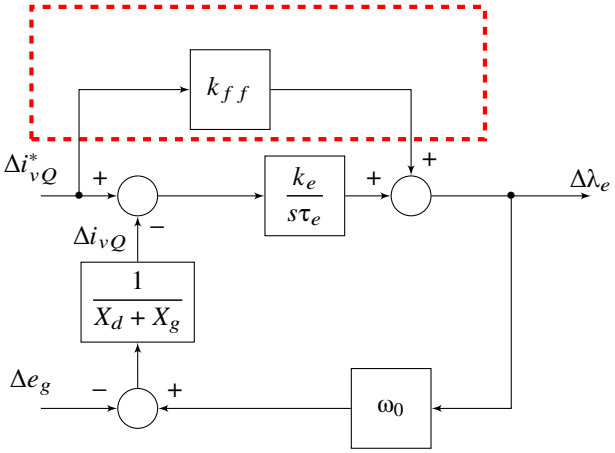


Figure 5. Block diagram of the excitation control of the VSM connected to the grid with feed-forward on the excitation flux linkage. The proposed feed-forward term is highlighted in red.

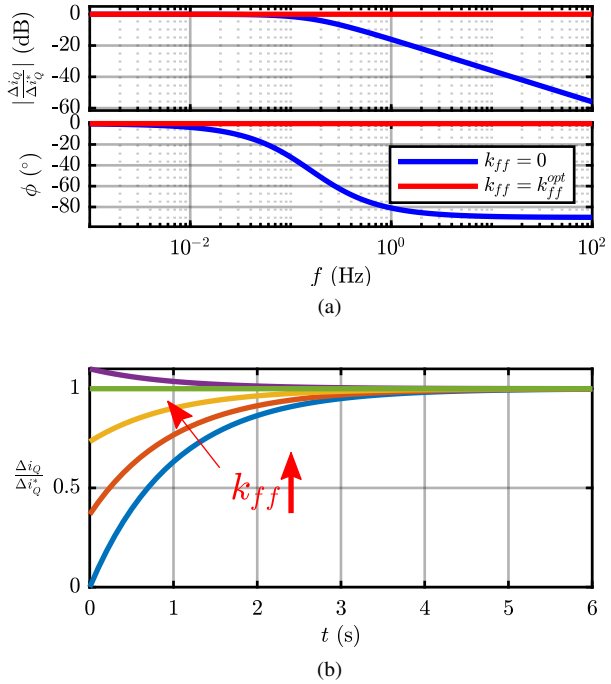


Figure 6. Theoretical behavior of the reactive current control. From top to bottom:
a) Bode diagram of the transfer function of the reactive current control with and without the optimal feed-forward $k_{ff} = k_{ff}^{opt}$;
b) Step response of the reactive current control for different values of $k_{ff} = \left[0 \ldots 1.1 k_{ff}^{opt}\right]$.

To study the effect of this feed-forward action, the following transfer function is considered:

$$\begin{aligned} G_{ff} &= \left.\frac{\Delta i_Q}{\Delta i_Q^*}\right|_{\Delta e_g = 0} = \frac{1 + k_{ff} F_e}{1 + L_g F_e} \\ F_e &= \frac{\tau_e s}{(X_d + X_g)\tau_e \omega_0 s + k_e} \end{aligned} \tag{10}$$

The optimal feed-forward term $k_{ff}^{opt}$ can be calculated by

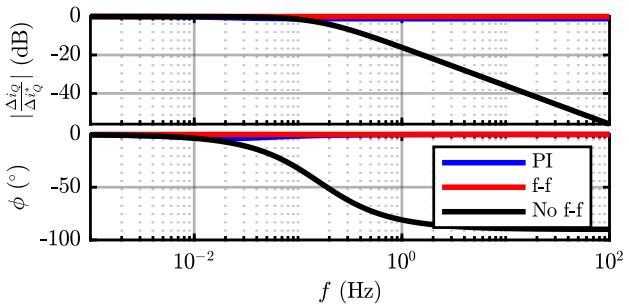


Figure 7. Comparison of the closed loop transfer function of the reactive control with a PI controller and with the proposed feed-forward control. The PI is an effective solution in tracking the steady state reactive reference. $k_p = 1$.

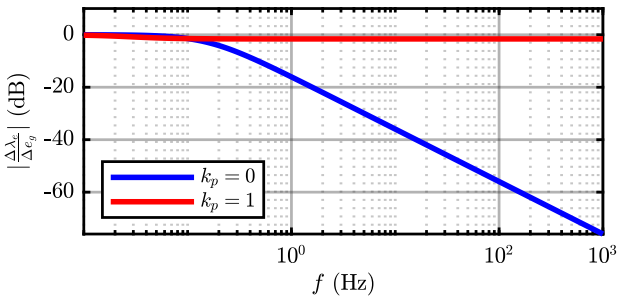


Figure 8. Grid disturbances amplitude rejection. When using a PI controller, there is a limited rejection of high frequency grid disturbances, such as harmonics. The proposed feed-forward control is immune to such disturbances.

imposing $G_{ff} = 1$ when $s \to \infty$ (instantaneous response to a step variation) and it results in $k_{ff} = k_{ff}^{opt} = \omega_0 (X_d + X_g)$. Fig. 6a shows the different frequency behavior with and without the proposed feed-forward ($k_{ff} = k_{ff}^{opt}$). It must be noted that the high frequency behavior is significantly improved with the proposed feed-forward. This benefit is even more evident in the simulated step response of the excitation control, shown in Fig. 6b. Several $k_{ff}$ have been tested and it is evident that with the optimal feed-forward $k_{ff}^{opt}$ the dynamic response is only influenced by the bandwidth of the internal current regulator (approximated to infinite in this analysis).

In order to highlight better the superiority of the proposed feed-forward control, a comparison with a PI-based solution is carried out. The regulator block $k_e/s\tau_e$ is replaced by the following:

$$PI(s) = k_p + \frac{k_e}{s\tau_e} \tag{11}$$

and the feed-forward is removed. The closed loop transfer function $\Delta i_Q/\Delta i_Q^*$ is calculated in three cases:

1) PI regulator (case PI);
2) Integral regulator with the proposed feed-forward (case f-f);
3) Integral regulator with no feed-forward (case No f-f).

In Fig. 7 these three cases are compared. As it can be seen, the PI and f-f regulators show an almost identical dynamic behavior. Both solutions are therefore suitable to obtain a fast reactive current regulation. On the other hand, the case no f-f relies only on a integral controller. Therefore, its dynamic response is quite slow. This case is the most similar to conventional synchronous generators, where the dynamic behavior of the excitation winding acts as a bottleneck for the reactive control.

The second term of comparison is the rejection to grid disturbances. This quantifies how sensitive is the reactive control to disturbances present in the grid, which are measured by the converter. Example of such disturbances are harmonics and measurement noise. For this aspect, it is preferable to have a high rejection of the high frequency input $\Delta e_g$. Therefore, the transfer function $\Delta\lambda_e/\Delta e_g$ is obtained and depicted in Fig. 8. As shown in the figure, the PI case has a limited high frequency rejection, that uniquely depends on the chosen

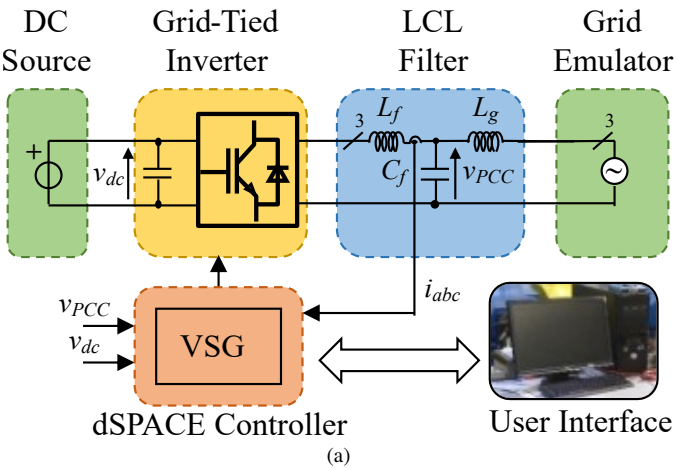


(a)

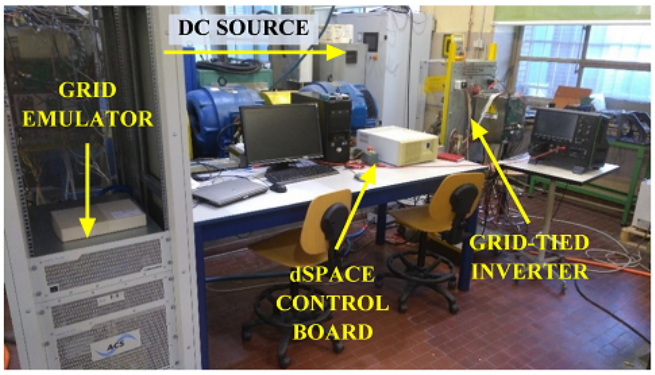


(b)

Figure 9. Experimental setup. From left to right:
a) Block diagram of the experimental setup;
b) Picture of the experimental setup.

proportional gain. On the other hand, the proposed feed-forward solution ($k_p = 0$) is immune from high frequency disturbances. This means that the proposed reactive controller will act uniquely in the positive fundamental sequence (DC in the virtual rotor $(d,q)$ rotating frame), rejecting any higher frequency disturbance.

## IV. Experimental Validation

A 15 kVA two-level three-phase $S_{base} = 15$ kVA inverter controlled at 10 kHz by a dSpace 1005 platform has been used

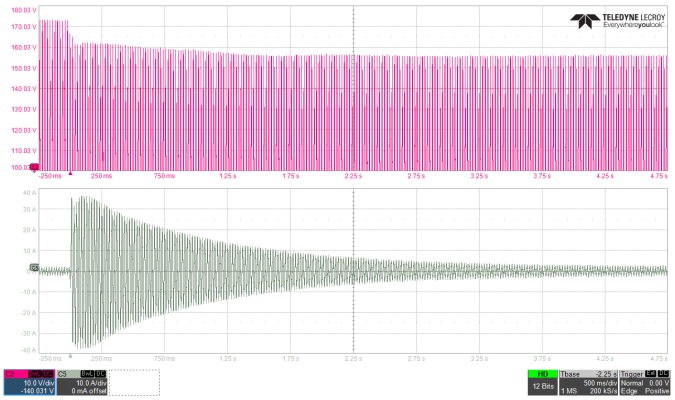

(a)

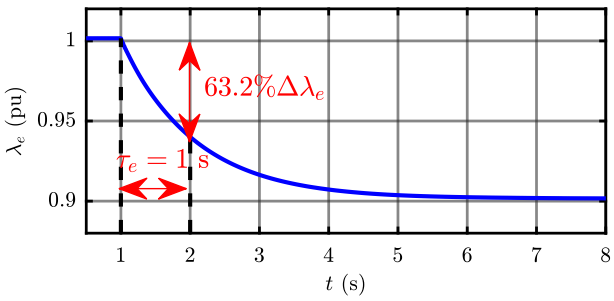


(b)

Figure 10. Test 1. A permanent voltage dip of -10% has been applied. The reference current vector is limited to 36 A peak to protect the inverter. From top to bottom:
a) Scope capture of the positive envelope of the grid phase voltage $a$ across $C_f$ (upper plot, Ch2) and of the injected grid current, phase $a$ (bottom plot, Ch5);
b) Transient behavior of the virtual excitation flux $\lambda_e$. The time constant $\tau_e$ = 1 s of the excitation control is highlighted graphically.

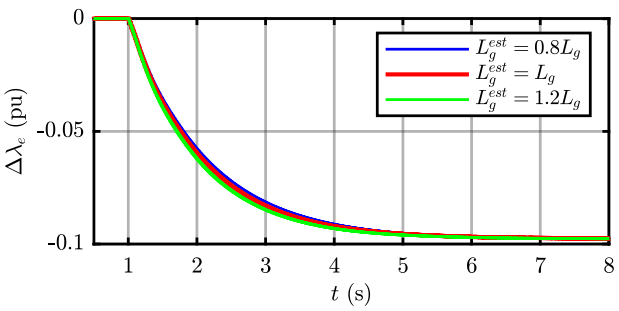


(a)

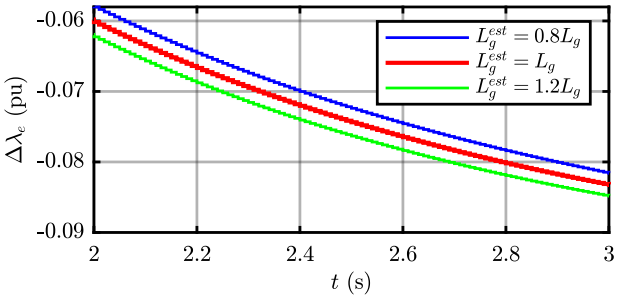


(b)

Figure 11. Test 2. A permanent voltage dip of -10% has been applied. The reference current vector is limited to 36 A peak to protect the inverter. The estimate grid impedance $L_g^{est}$ varies from $0.8L_g$ to $1.2L_g$. From top to bottom:
a) Variation of the virtual excitation flux $\Delta\lambda_e$;
b) Detail of to highlight the differences due to a non ideal estimation $L_g^{est}$ of the grid inductance.

for experimental validation. The experimental setup is depicted in Fig. 9. This inverter is connected to a grid emulator (rated 50 kVA and emulating a 120 Vrms phase voltage grid at 50 Hz) through an LCL filter ($L_f$ = 545 µH, $C_f$ = 22 µF and $L_{fg}$ = 120 µH). A known grid impedance of $L_g$ = 270 µH is placed between the inverter and the grid emulator. The VSM virtual stator reactance $X_d$ = 0.1 pu and the excitation control time constant $\tau_e$ = 1 s. The DC side is a constant power supply $v_{dc}$.

The grid side converter behaves as a current source (as in Fig. 1). The current controller is a PI implemented in the rotating ($d$,$q$) frame synchronous with the virtual rotor of the machine ($\theta_r$). Besides, a resonant controller tuned to the sixth harmonic in the same ($d$,$q$) frame have been added. It must be noted that any current control scheme is suitable for this application. The only requirement is that the current control bandwidth must be sufficiently larger than the time constant $\tau$ of the excitation control. This is usually the case, being $\tau$ in the order of magnitude of seconds. In this work, the current control bandwidth has been set to 800 Hz.

Two perturbations have been applied to the system:

1) Permanent voltage dip. First, Test 1 validates the tuning procedure of the excitation control. Then, Test 2 validates the effect of an incorrect grid inductance estimation on the reactive control.
2) Step in the reactive current reference of the inverter. Test 3 validates the effectiveness of the proposed feed-forward term, while Test 4 analyses the effects of an incorrect estimation of the grid inductance on the optimal feed-forward coefficient $k_{ff}^{opt}$.

In Test 1 (Fig. 10) a permanent voltage dip (-10%) is applied. The time constant of the excitation control is set to $\tau_e$ = 1 s. The time constant is defined as the time span needed to complete 63.2% of the transient. In the considered case, the transient is 0.1 pu, therefore, the time constant $\tau$ can be measured by calculating the time between the beginning of the transient until $\lambda_e$ = 0.9368 pu. From the measurement of the transient response, this time constant $\tau_e$ can be measured and corresponds to the desired value of 1 s.

In Test 2 the same permanent voltage dip (-10%) is applied as in Test 1. As it is shown in Fig. 11, the behavior excitation flux linkage variation is loosely dependent on the estimation of the grid inductance. An estimation error of ±20% does not seriously affect the time constant tuning. Therefore, the proposed tuning procedure can be considered valid also under incorrect grid inductance estimation or variations due to faults or grid reconfigurations.

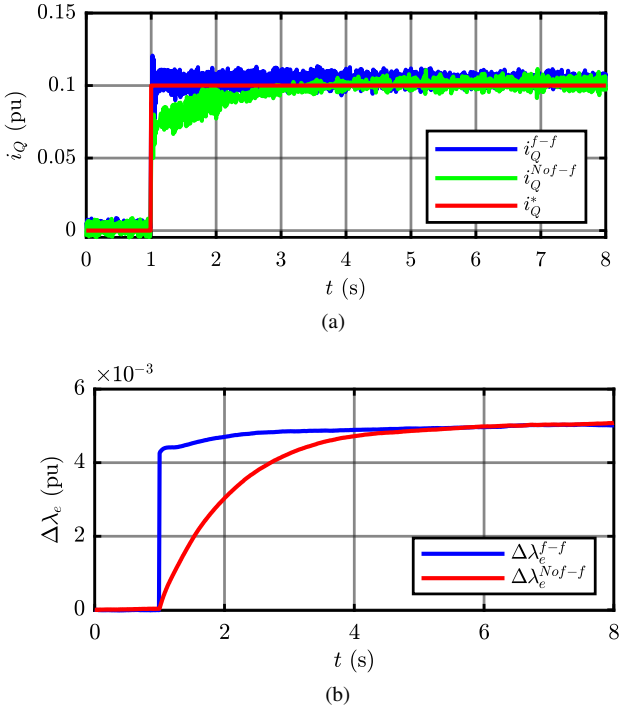


Figure 12. Test 3. A step of 0.1 pu in the reactive current reference is applied (from 0 to 0.1 pu). From top to bottom:
a) Reactive current reference $i_Q^*$ and actual reactive current value $i_Q$ with and without the optimum feed-forward $k_{ff} = k_{ff}^{opt}$;
b) Virtual excitation flux variation $\Delta\lambda_e$ with and without the optimum feed-forward $k_{ff} = k_{ff}^{opt}$.

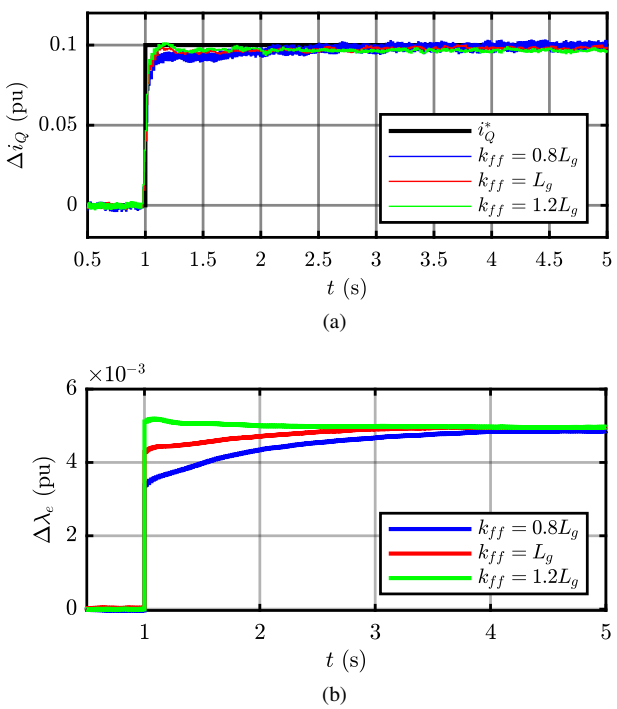


Figure 13. Test 4. A step of 0.1 pu in the reactive current reference is applied. The feed-forward gain $k_{ff}$ varies from $0.8L_g$ to $1.2L_g$. From top to bottom:
a) Reactive current reference $i_Q^*$ and actual reactive current value $i_Q$ with various feed-forward gains $k_{ff}$;
b) Virtual excitation flux variation $\Delta\lambda_e$ with various feed-forward gains $k_{ff}$.

In Test 3 (Fig. 12), a step of 0.1 pu in the reactive current reference is applied. The behavior of the system is compared with and without the optimal feed-forward term $k_{ff} = L_g$. The action of the feed-forward adapts instantly the flux linkage $\lambda_e$ to the value after transient. This way, the transient is much shorter than the one that would result without such feed-forward control. Moreover, this transient is only related to the inner current controller and not to the excitation time constant $\tau_e$, which is only in charge of regulating the reactive support during voltage dips. As it can be seen if Fig. 12b, the excitation flux $\lambda_e$ does not reach exactly the final value after the step with to the feed-forward. The estimation of the grid impedance is not ideal and therefore a small error is always present. However, such error is compensated by the integral action of the excitation control.

## V. Conclusion

This paper demonstrated how the tuning of the excitation control of a VSM depends both on the virtual stator and the grid reactances and proposes a simple tuning formula of the excitation control gain $k_e$. This $k_e$ depends on the machine and grid parameters, therefore it is important to carefully estimate the grid impedance. Moreover, a feed-forward term is proved as an effective solution to increase the dynamic behavior of the reactive current control, decoupling the time constant of the reactive support during voltage dips from the one of the inner current controller when changing the reference of reactive power. This guarantees a fast dynamic response when modifying the converter reactive power references, while being more immune than a PI regulator to measurement disturbances, such as harmonics or unbalance. As demonstrated both theoretically and experimentally, the proposed tuning procedure and feed-forward term are robust to incorrect grid inductance estimation or variations due to faults or grid reconfigurations. Moreover, the error in the estimation of the grid impedance are affecting the response only transiently and are compensated by the steady-state integral action of the excitation control.

## References


[1] H. Beck and R. Hesse, "Virtual synchronous machine," in *2007 9th International Conference on Electrical Power Quality and Utilisation*, Oct. 2007, pp. 1–6.

[2] S. D'Arco, J. A. Suul, and O. B. Fosso, "A Virtual Synchronous Machine implementation for distributed control of power converters in SmartGrids," *Electric Power Systems Research*, vol. 122, pp. 180–197, May 2015.

[3] P. Rodríguez, C. Citro, J. I. Candela, J. Rocabert, and A. Luna, "Flexible Grid Connection and Islanding of SPC-Based PV Power Converters," *IEEE Transactions on Industry Applications*, vol. 54, no. 3, pp. 2690–2702, May 2018.

[4] H. Bevrani, T. Ise, and Y. Miura, "Virtual synchronous generators: A survey and new perspectives," *International Journal of Electrical Power & Energy Systems*, vol. 54, pp. 244–254, Jan. 2014.

[5] Q.-C. Zhong and G. Weiss, "Synchronverters: Inverters That Mimic Synchronous Generators," *IEEE Trans. Ind. Electron.*, vol. 58, no. 4, pp. 1259–1267, Apr. 2011.

[6] M. van Wesenbeeck, S. de Haan, P. Varela, and K. Visscher, "Grid tied converter with virtual kinetic storage," in *2009 IEEE Bucharest PowerTech*. Bucharest: IEEE, Jun. 2009, pp. 1–7.

[7] Y. Hirase, K. Abe, K. Sugimoto, and Y. Shindo, "A grid-connected inverter with virtual synchronous generator model of algebraic type," *Elect. Eng. Jpn.*, vol. 184, no. 4, pp. 10–21, Sep. 2013.

[8] W. Zhang, A. Tarraso, J. Rocabert, A. Luna, J. I. Candela, and P. Rodriguez, "Frequency Support Properties of the Synchronous Power Control for Grid-Connected Converters," *IEEE Trans. on Ind. Applicat.*, vol. 55, no. 5, pp. 5178–5189, Sep. 2019.

[9] T. Shintai, Y. Miura, and T. Ise, "Oscillation Damping of a Distributed Generator Using a Virtual Synchronous Generator," *IEEE Trans. Power Delivery*, vol. 29, no. 2, pp. 668–676, Apr. 2014.

[10] L. Zhang, L. Harnefors, and H.-P. Nee, "Power-Synchronization Control of Grid-Connected Voltage-Source Converters," *IEEE Trans. Power Syst.*, vol. 25, no. 2, pp. 809–820, May 2010.

[11] F. Mandrile, E. Carpaneto, and R. Bojoi, "Grid-Tied Inverter with Simplified Virtual Synchronous Compensator for Grid Services and Grid Support," in *2019 IEEE Energy Conversion Congress and Exposition (ECCE)*. Baltimore, MD, USA: IEEE, Sep. 2019, pp. 4317–4323.

[12] L. Asiminoaei, R. Teodorescu, F. Blaabjerg, and U. Borup, "Implementation and Test of an Online Embedded Grid Impedance Estimation Technique for PV Inverters," *IEEE Trans. Ind. Electron.*, vol. 52, no. 4, pp. 1136–1144, Aug. 2005.

[13] T. Roinila and T. Messo, "Online Grid-Impedance Measurement Using Ternary-Sequence Injection," *IEEE Trans. on Ind. Applicat.*, vol. 54, no. 5, pp. 5097–5103, Sep. 2018.

[14] A. V. Timbus, P. Rodriguez, R. Teodorescu, and M. Ciobotaru, "Line Impedance Estimation Using Active and Reactive Power Variations," in *2007 IEEE Power Electronics Specialists Conference*. Orlando, FL, USA: IEEE, 2007, pp. 1273–1279.

[15] A. Vidal, A. G. Yepes, F. D. Freijedo, O. Lopez, J. Malvar, F. Baneira, and J. Doval-Gandoy, "A Method for Identification of the Equivalent Inductance and Resistance in the Plant Model of Current-Controlled Grid-Tied Converters," *IEEE Trans. Power Electron.*, vol. 30, no. 12, pp. 7245–7261, Dec. 2015.

[16] J. Kukkola, M. Routimo, and M. Hinkkanen, "Real-Time Grid Impedance Estimation Using a Converter," in *2019 IEEE Energy Conversion Congress and Exposition (ECCE)*. Baltimore, MD, USA: IEEE, Sep. 2019, pp. 6005–6012.